Coherence properties of exciton polariton OPO condensates in one and two dimensions

2012 New J. Phys. 14 075018

New Journal of Physics
The open-access journal for physics

Coherence properties of exciton polariton OPO condensates in one and two dimensions

R Spano[1,5,6], J Cuadra[1], G Tosi[1], C Antón[1,2], C A Lingg[1], D Sanvitto[1,7], M D Martín[1,2], L Viña[1,2], P R Eastham[3], M van der Poel[4] and J M Hvam[4]

[1] Dept. Física Materiales, Universidad Autonóma de Madrid, Madrid 28049, Spain
[2] Instituto de Ciencia de Materiales 'Nicolás Cabrera', Universidad Autónoma de Madrid, Madrid 28049, Spain
[3] School of Physics, Trinity College Dublin, College Green, Dublin 2, Ireland
[4] DTU Fotonik, Tech. Univ. Denmark, Orsteds Plads 343, DK-2800 Kgs. Lyngby, Denmark
E-mail: rita.spano@uam.es

New Journal of Physics **14** (2012) 075018 (13pp)
Received 14 March 2012
Published 20 July 2012
Online at http://www.njp.org/
doi:10.1088/1367-2630/14/7/075018

Abstract. We give an overview of the coherence properties of exciton–polariton condensates generated by optical parametric scattering. Different aspects of the first-order coherence ($g^{(1)}$) have been investigated. The spatial coherence extension of a two-dimensional (2D) polariton system, below and at the parametric threshold, demonstrates the development of a constant phase coherence over the entire condensate, once the condensate phase transition takes place. The effect on coherence of the photonic versus excitonic nature of the condensates is also examined. The coherence of a quasi-1D trap, composed of a line defect, is studied, showing the detrimental effect of reduced dimensionality on the establishment of the long range order. In addition, the temporal coherence decay, $g^{(1)}(\tau)$, reveals a fast decay in contrast with the 2D case. The situation of a quasi-1D condensate coexisting with a 2D one is also presented.

[5] Author to whom any correspondence should be addressed.
[6] Present address: Laboratoire d'Optoélectronique Quantique, École Polytechnique Fédérale de Lausanne (EPFL), Station 3, CH-1015 Lausanne, Switzerland.
[7] Present address: NNL, Istituto Nanoscienze—CNR and Istituto Italiano di Tecnologia, IIT-Lecce, Lecce, Italy.

Contents

1. Introduction

The exciton–polaritons described in this work are quasi-particles emerging from the strong coupling between the photonic mode of a high-finesse microcavity and the excitonic mode of a quantum well (QW) structure embedded in the microcavity [1]. As these particles arise from a photon–exciton mixed state, they have a bosonic nature and can undergo a Bose–Einstein-like phase transition. Over the last two decades, the interest of the scientific community in polariton properties has grown exponentially, especially after the experimental demonstration of polariton condensation in 2006 [2]. Their mixed nature gives them some unique properties; as an example the photonic component of polaritons is responsible for their light mass, of the order of 10^{-4} times the electron mass, that allows for a transition to the condensate phase to take place at liquid He [2], up to room temperature [3]. Moreover, the one-to-one correspondence between the microcavity polaritons and the photons escaping from the cavity makes possible a complete characterization of polariton properties only by means of spectroscopic measurements. As they have a very short lifetime, mainly due to the microcavity photon losses, only a quasi-equilibrium condensation is possible, where a stationary state is reached when a driving pump can compensate for the polariton losses of the condensate. All these characteristics make polaritons unique particles, compared to atomic equilibrium condensates, to investigate new aspects of condensation, such as superfluidity and hydrodynamics [4–8]. Only recently, polaritons have been proposed for application in optoelectronic devices, and some properties suitable for application such as spin-switching effects [9–11] have already been demonstrated.

On the other hand, the excitonic component of polaritons gives rise to two-body interactions, which permit the observation of scattering phenomena. One of the most studied effects related to polariton interactions is the optical parametric oscillator (OPO), a strong $\chi^{(3)}$-type nonlinear effect, stronger than that in nonlinear optical bulk crystals [12], that permits an efficient conversion of two pump polaritons into a pair of signal and idler polaritons. The OPO effect in microcavities was demonstrated in 2000 simultaneously by two groups [13, 14], who achieved a massive occupation of the signal and idler states by this resonant pumping scheme. Polariton condensation has been demonstrated by both nonresonant and resonant (OPO) optical excitation techniques. In both cases massive occupation of a low-energy state takes place and a macroscopic wavefunction (the order parameter of the system) with a well-defined phase is needed to describe the state. The phase transition is experimentally evidenced by, among other effects, the narrowing of the emission in energy and momentum space. The counterpart in Fourier space of the energy and momentum narrowing is, by the Wiener–Khinchin identity [15–17], an extended spatial and temporal coherence in real space [17, 18], which explains why the appearance of such coherence in both resonantly [19]

and non-resonantly [2, 20] created condensates has been investigated as a fingerprint of condensation. In particular, the pioneering work of Baas *et al* [19] shows for the first time that a very extended spatial coherence can be achieved in an OPO condensate. One has to also keep in mind that microcavity polaritons constitute a two-dimensional (2D) system and that in infinite 2D systems a true Bose-Einstein condensation (BEC) transition cannot take place [17, 21], and a power-law decay of the spatial coherence is expected instead. However, in a finite condensate such power-law decay may be on scales longer than the decay of the condensate, so that spatially uniform coherence could be observed. Furthermore, the coherence observed for the OPO is spontaneous and not inherited from the pump [22–24]. In fact, the only constraints in the parametric process are the phase matching conditions, i.e. the energy and momentum conservation $2\omega_p = \omega_s + \omega_i$ and $2k_p = k_s + k_i$, where $\omega_{p,s,i}$ and $k_{p,s,i}$ are the energies and momenta of the pump, signal and idler, respectively. These phase-matching conditions lock the overall phases of the signal and idler to that of the pump, but leave a free relative phase that is spontaneously broken. The effects of spatial fluctuations in this phase in the OPO polariton condensate have been addressed in a theoretical work by Carusotto and Ciuti [25]. They studied the coherence of the OPO tuning the pump frequency below and above the parametric threshold, E_{Th}, which is the energy at which the OPO takes place once the other parameters, such as pump angle and power, are set. One should note that the threshold in this theoretical work is established by the energy mismatch, ϵ, between that of the excitation laser and that needed to fulfill the phase-matching conditions, and not by the pump power needed for obtaining stimulated scattering to the signal, as more generally used in the literature, and that the same approach will be used in this paper. The numerical results show the development of a constant phase coherence for a finite 2D OPO condensate, once the parametric scattering threshold is reached at E_{Th} ($\epsilon = 0$), and a spatially decaying coherence when exciting below the threshold ($\epsilon < 0$) for which the condensation by parametric scattering is not efficiently established. In the same work, they present a preliminary study of the coherence properties of a 1D OPO system, where the coherence is expected to decay rapidly along the condensate length even when pumping at the parametric threshold, E_{Th}. For atomic condensates, which are equilibrium systems, the theory developed in [17] for the 1D case predicts an exponential decay of the phase coherence. In the case of polariton condensates, which are instead out of equilibrium, the theory does not necessarily hold anymore. Such a non-trivial theoretical issue of coherence of OPO condensates generated in 1D systems has been further developed in a subsequent work of Wouters and Carusotto [26], who predicted the coherence behavior by means of numerical simulations. For the 1D system they found that the effects of long-wavelength fluctuations are expected to be stronger than those in the 2D case, being able to destroy the long-range order [17, 26]. For these systems, in the case of an ideal disorder-less scenario, they predict that the spatial coherence along the 1D condensate direction (y) decays with an exponential law: $g^{(1)}(y) \propto e^{-|y|/l_c}$, with l_c being the coherence length, which they estimate to be of the order of a few hundreds of microns. The coherence degree of 1D condensates has also been addressed in a recent work of Malpuech and Solnyshkov [27], in which they take into account the presence of disorder; in this case they predict a fluctuating degree of coherence in space, with the maxima of coherence in correspondence to potential minima.

In this work, we first recall the coherence properties of a 2D condensate below ($\epsilon < 0$) and at ($\epsilon = 0$) the parametric threshold, where we find [28] an extended coherence at threshold (figure 2), as predicted in [25]. We show that moving away from threshold can lead either to complete loss of coherence or to the formation of a weak fluctuating condensate coexisting with

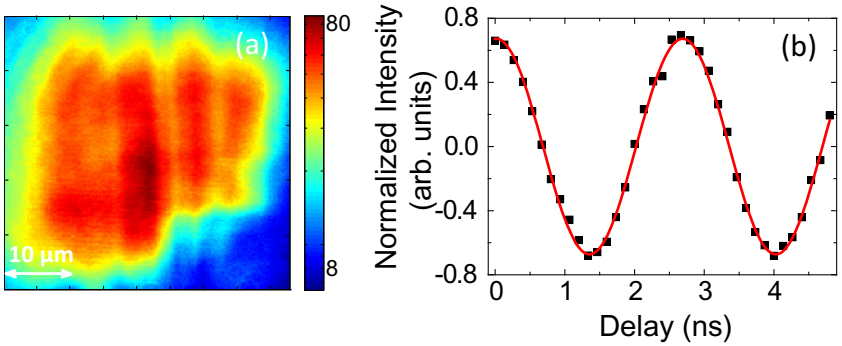

Figure 1. (a) Typical real-space emission intensity (false color scale) from the signal condensate generated by OPO at a detuning $\Delta E = -4$ meV. (b) Sinusoidal evolution of the normalized emission (I_{Norm}) versus the delay of a Mach–Zender-interferometer retro-reflector arm. The red line is a sinusoidal fit.

a population of incoherent polaritons (figure 3). We then investigate the 1D OPO coherence in line defects present in the sample. The spatial coherence is found to decay rapidly along the line defects even under resonant pumping, with a modulation due to the potential landscape of the sample (figure 8). This reflects the dominant role of disorder in determining the coherence length of these low-dimensional condensates.

2. Spatial coherence of a two-dimensional (2D) condensate

One of the most detrimental effects in the measurement of coherence is the noise coming from the laser source, which can mask the mode structure of the condensate and enlarges artificially the emission energy linewidth. In order to avoid these effects, we use a CW monomode laser, with a very narrow bandwidth of 75 kHz, to carry out the OPO experiments on a high-quality λ-microcavity grown by molecular beam epitaxy. The sample we used has a single 10 nm $GaAs/Al_{0.3}Ga_{0.7}As$ QW placed at the antinode of the cavity. The top/bottom Bragg mirror structure is made of 16 (25) periods of $\lambda/4$ $AlAs/Al_{0.15}Ga_{0.85}As$ layers. The Rabi splitting is $2\hbar\Omega = 4.2$ meV and a wedge of the cavity permits us to make measurements from negative up to positive detunings (the detuning, ΔE, is defined as the difference between the bare cavity and exciton energies). We create a condensate with a large diameter, of about $\sim 40\,\mu$m, in order to investigate the coherence properties of a true 2D condensate. We manage to have such an extended condensate area by exciting the sample with a large-diameter Gaussian laser beam. In order to obtain parametric scattering, we pump the lower polariton branch (LPB) close to its inflection point at a power level that permits the development of stimulated scattering processes, generating pairs of signal and idler polaritons, and maintaining the temperature of the sample at 10 K. The characteristics of the condensate phase are investigated both in the real-space emission as depicted in figure 1(a) and in the Fourier space emission, as depicted in figures 2(a)–(c).

As can be seen from the real-space image of figure 1(a), a bright emission from the entire condensate area appears when we set the laser energy at $E_{\mathrm{Th}} = 1552.4$ meV ($\epsilon = 0$). When we look at the Fourier space, we pass from a broad distribution in energy and momentum far from the threshold, $\epsilon \gg 0$ (figure 2(a)), indicating that a wide range of available states are occupied,

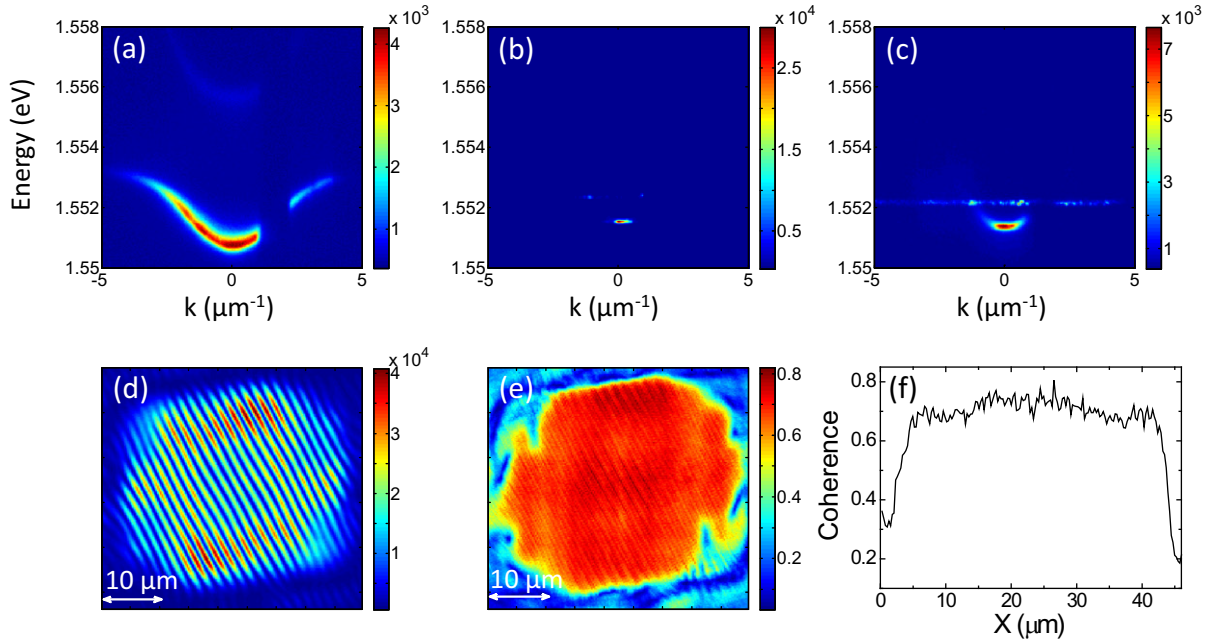

Figure 2. (a) Typical energy versus k dispersion of the lower and upper polariton branches for the 2D microcavity polariton system, the detuning is $\Delta E = -4$ meV and the measurement is obtained pumping far above from the inflection point, $E = 1642$ meV. (b) k-space emission at the parametric threshold, $E_{\mathrm{Th}} = 1552.4$ meV, when the parametric scattering (OPO) takes place generating a condensate at $E_{\mathrm{OPO}} = 1551.5$ meV with a blueshift of $\delta E = 1$ meV. (c) k-space emission when the pump is redshifted by 0.2 meV from E_{Th}. (d) Interference pattern of a condensate created by OPO at the parametric threshold with a pump power density $P_{\mathrm{D}} = 1.7\,\mathrm{kW\,cm^{-2}}$, and (e) the corresponding coherence map extending over a distance of $d = 44\,\mu$m. (f) The horizontal profile taken at the center of the condensate map, showing constant coherence along the condensate region.

to a very narrow distribution at OPO threshold (E_{Th}) (figure 2(b)), indicating that a massive occupation of the $k = 0$ state takes place, with a consequent blueshift of the order of $\delta = 1$ meV. When we further redshift the driving pump by $\epsilon = -0.2$ meV, we observe a broadening in both the energy and momentum emission and a decrease of the blueshift (figure 2(c)).

To investigate the coherence of the signal emission in real space, we use a Mach–Zehnder interferometer in the retro-reflector configuration. One arm of the interferometer is equipped with a retro-reflector mirror, which flips the condensate image in a center symmetric way. Combining at the output of the interferometer both the real image and its center symmetric counterpart, we can evaluate from the resulting interference pattern the phase of each point (x, y) of the condensate with respect to the phase of its opposite counterpart $(-x, -y)$. This procedure permits access to the first-order coherence function $g^{(1)}[(x, y), (-x, -y)] = \frac{\langle E^*(x,y)E(-x,-y)\rangle}{\langle E^*(x,y)\rangle\langle E(-x,-y)\rangle}$ [2, 18] at each point of the condensate. In order to obtain the coherence map of the entire condensate from the interference pattern, we move the retro-reflector arm by nanometer steps adding a small delay: the interference between the two

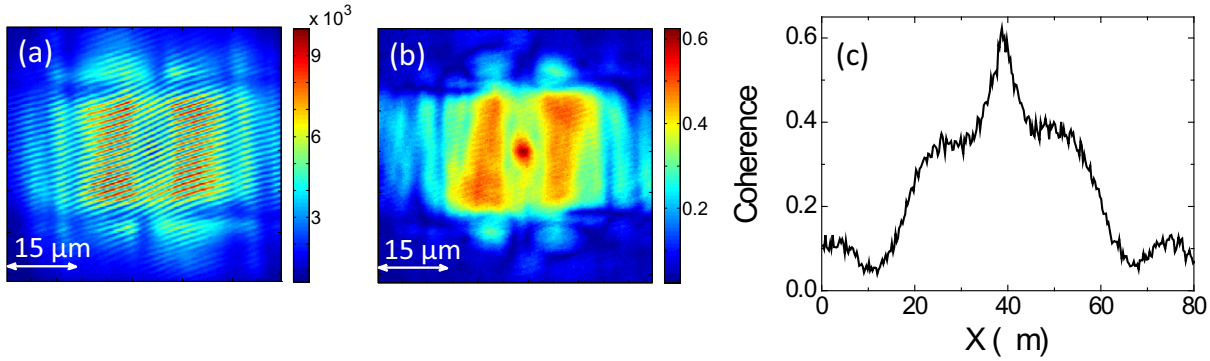

Figure 3. (a) Interference pattern for a detuning $\Delta E = -4$ meV and (b) coherence map from the polariton emission when the pump is redshifted by 0.2 meV with respect to E_{Th} in pump power conditions for having the OPO. (c) Horizontal profile taken at the middle of the coherence map, showing a decaying coherence at the center of the emission area, corresponding to an incoherent polariton population, and a flat and lower coherence on the sides, corresponding to the buildup of the condensate population.

arms passes from constructive to destructive gradually, giving a sinusoidal modulation to the intensity as a function of the delay (figure 1(b)). To extract the coherence, we use the following normalized expression: $I_{\mathrm{Norm}}[(x, y), (-x, -y)] = \frac{I_{\mathrm{Tot}} - I_{\mathrm{RR}} - I_{\mathrm{M}}}{2\sqrt{I_{\mathrm{RR}} I_{\mathrm{M}}}} = g^{(1)}[(x, y), (-x, -y)] \sin(\omega \Delta t + \varphi_0)$, where I_{Tot} is the total intensity of the interference pattern, I_{RR} (I_{M}) is the intensity recorded from the arm with the retro-reflector (single mirror), ω is the frequency of the periodic pattern of the interference fringes and φ_0 is a constant phase of the condensate. Repeating this procedure for each point we reconstruct the entire coherence map.

The momentum and energy narrowing at the OPO threshold corresponds to the development of a macroscopic coherence in the real space as depicted in figures 2(d)–(f), and highlighted by the horizontal profile taken at the center of the condensate emission, showing a constant coherence extending along the whole condensate area, validating the predictions of Carusotto and Ciuti [25].

When moving from E_{Th} toward lower energies, two possible scenarios can happen: (i) a fast exponential decay along the condensate area as predicted in [25] and demonstrated in [28] (see figure 1(f) of [28]), or (2) a hybrid situation as presented in figures 3(a)–(c) where a rapid exponential decay is superimposed on the top of a flat and lower coherence region. In the latter case, the exponential part that decays within a few de Broglie wavelengths, as better depicted by the horizontal profile shown in figure 3(c), is related to uncondensed polaritons, and the higher degree of coherence at the center is due to the autocorrelation of the center with itself. The flat part with a moderate degree of coherence is instead related to the nucleation of the condensate, which is developing a constant phase.

The detuning, ΔE, between the excitonic and photonic modes determines the excitonic fraction and the interaction strength between polaritons. For negative detunings the photonic fraction is higher and the interactions are expected to be lower, which could be attributed as the cause of the extended coherence. In order to demonstrate that the observed large coherence

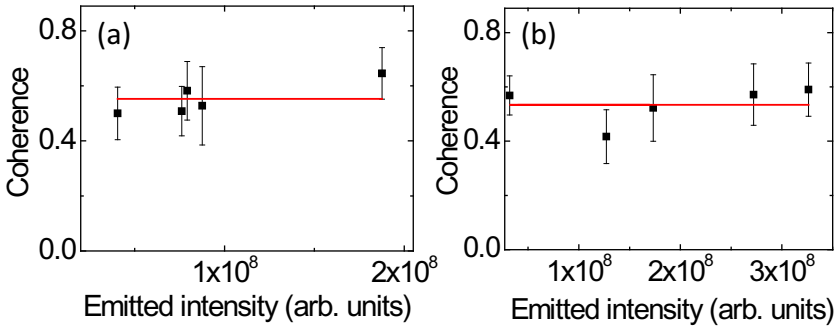

Figure 4. (a) Coherence as a function of integrated emitted intensity at zero detuning, corresponding to an interval of pump powers spanning from $P = 40\,\mathrm{mW}$ up to $P = 120\,\mathrm{mW}$ and to a condensate area increasing with an increase of the pump power, from $A = 1.4 \times 10^3\,\mu\mathrm{m}^2$ up to $A = 2.3 \times 10^3\,\mu\mathrm{m}^2$. (b) Coherence as a function of integrated emitted intensity at the negative detuning $\Delta E = -3.6\,\mathrm{meV}$, corresponding to the same pump power range, which corresponds to a condensate area increasing from $A = 3 \times 10^3\,\mu\mathrm{m}^2$ up to $A = 3.3 \times 10^3\,\mu\mathrm{m}^2$. At both detunings the degree of coherence is similar. For each measurement and at each detuning the phase matching conditions for the parametric scattering are fulfilled. (The straight lines are a guide to the eyes.)

length is not due to the photonic nature of the condensate at the negative detuning at which we make the coherence measurements, we have repeated our experiment (not shown here) at zero detuning, and we still observed the same large spatial coherence extension. Moreover, for both detunings we studied the degree of coherence as a function of pump power, which corresponds to increasing emission of the condensate. As an increment of pump power implies a larger blueshift, at each measurements we adjusted the pump energy and angle in order to fulfill the requirements for achieving OPO conditions. Figures 4(a) and (b) depict the degree of coherence as a function of the emitted intensity of the condensate (which corresponds to increasing pump power) for both zero (a) and negative detuning of $\Delta E = -3.6\,\mathrm{meV}$ (b). The average pump power at which the measurements were carried out spans from $P = 40\,\mathrm{mW}$ up to $P = 120\,\mathrm{mW}$ for both detunings. As the pump beam has a Gaussian profile an increase of the power implies a corresponding increase of the condensate area: in the case of the zero-detuning experiment the area goes from $A = 1.4 \times 10^3\,\mu\mathrm{m}^2$ at $P = 40\,\mathrm{mW}$ up to $A = 2.3 \times 10^3\,\mu\mathrm{m}^2$ at $P = 120\,\mathrm{mW}$; in the case of negative detuning, the condensate area is more stable with respect to the pump power; in fact it goes only from $A = 3 \times 10^3\,\mu\mathrm{m}^2$ at the lowest power up to $A = 3.3 \times 10^3\,\mu\mathrm{m}^2$ at the highest power. It is also worth noting that for larger negative detunings at the same pump power, condensates with larger areas are obtained. From these experiments it is clearly seen that almost the same degree of coherence is reached when the OPO condensate is created either at zero or at negative detunings. Moreover, the intensity dependence demonstrates that once the threshold for OPO condensation is reached, a stable state is established and the degree of coherence remains almost constant, showing only a small power dependence, as long as the system is in the strong coupling regime. The main difference between zero and negative detunings is that in the more excitonic case the strong coupling is lost at lower powers than those corresponding to the condensates with larger photonic content.

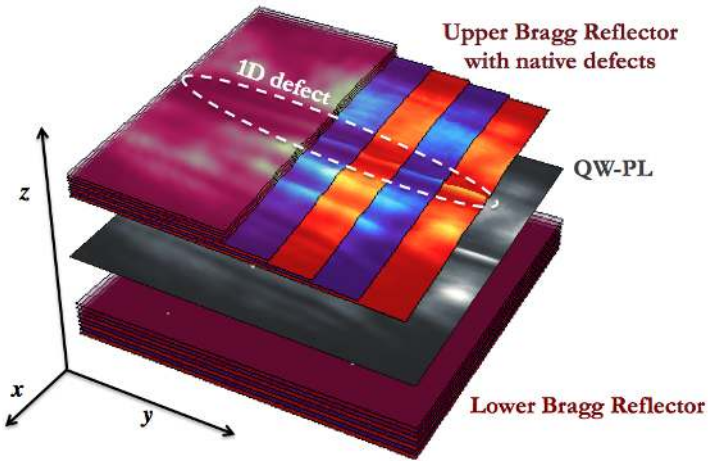

Figure 5. Schematic representation of the sample with a defect due to the imperfections of the top Bragg mirrors, developing along the y-direction, and resulting in the confinement along the x-direction.

3. 1D line-defect coherence compared to 2D coherence

As already mentioned in the introduction, we have also studied, at a negative detuning of $\Delta E = -4$ meV, the coherence properties of a line defect present on the sample. Plausibly, these defects originate from imperfections in the upper Bragg reflector, as sketched in figure 5. As observed under non-resonant weak excitation, the effect of this line defect, with a width of $x = 3\,\mu$m and a length of $y = 60\,\mu$m, is to confine the excitons and the light in the x-direction, in addition to the confinement in the z direction parallel to the growth direction provided by the QW and the cavity, respectively, resulting in a quasi-1D system. The result of this extra confinement is the opening of subbranches (not shown here), which can be observed in the energy–momentum space, where the line defect emission is at the energy $E_{1D} = 1546.2$ meV, 3.6 meV below the emission of the LPB.

We carry out the study of coherence in two different cases, (a) generating the OPO in the 1D, pumping at the inflection point of the 1D branch, and (b) generating the OPO in the 2D system, by phase matching the 2D branch. The results of this procedure are depicted in figures 6(a)–(d), where, using a dove prism, we are able to record the OPO emission along two directions, parallel and orthogonal to the line defect. Figure 6(a) shows the emission of the 1D-OPO condensate generated by pumping at the inflection point of its LPB (case (a)), tuning the pump laser at $E_{Th} = 1551.1$ meV and with an average power $P = 0.07$ W. The condensate emission coming from the direction k_x shows a flat dispersion due to the confinement along x. However, the emission coming from the direction k_y, parallel to the defect, exhibits a small curvature in its dispersion (see figure 6(b)). The dramatic effect of excitonic interactions is witnessed by the strong blueshift experienced by the emission energy of the line defect, of the order of $\delta E = 3.3$ meV. Tuning the laser toward higher energies and increasing the pump power from $P = 0.07$ W to $P = 0.1$ W, we phase match the 2D system at $E_{Th} = 1551.6$ meV (case (b)) achieving an OPO condensate as depicted in figure 6(c) for emission collected orthogonally to the line defect and 6(d) for parallel collection. In this case, the blueshift for the LPB of the 2D condensate is only $\delta E = 0.4$ meV, much lower than that of the 1D case, but the 1D

IOP Institute of Physics DEUTSCHE PHYSIKALISCHE GESELLSCHAFT

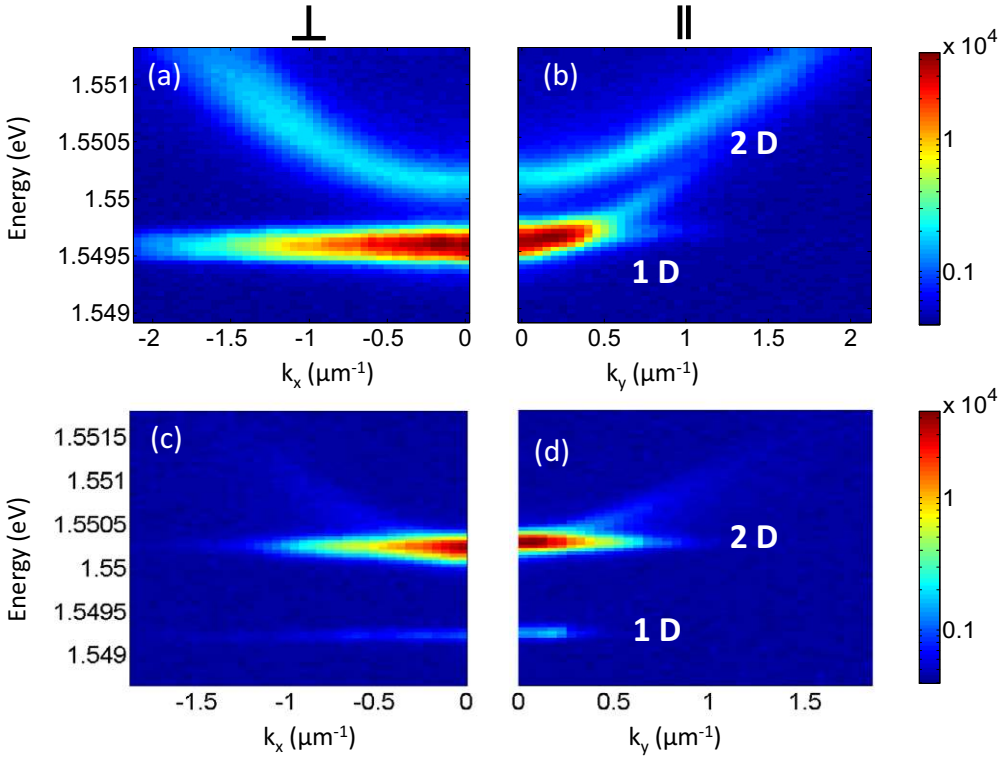

Figure 6. *k*-space OPO emission from the orthogonal (a) and parallel (b) directions to the line defect when phase matching the line defect at $E_{\mathrm{Th}} = 1551.1$ meV at the average pump power $P = 0.07$ W. The 1D emission shows a blueshift of $\delta E = 3.3$ meV when the OPO takes place. (c, d) Emission from the orthogonal and parallel directions to the defect, respectively, for the case of the OPO achieved by phase matching the 2D LPB. The pump laser is tuned at $E_{\mathrm{Th}} = 1551.6$ meV at a power $P = 0.1$ W. Both the 2D and 1D energy levels experience a blueshift of $\delta E = 0.4$ meV and $\delta E = 3.2$ meV, respectively, indicating that in this case the 2D and 1D systems are massively occupied.

system still experiences the same strong blueshift and shows a very narrow emission as when it was resonantly pumped, indicating that the line defect is still massively occupied and the condensation is still present.

Figures 7(a) and (d) display the real-space counterparts of the two cases presented in figure 6. When we phase match only the line defect energy dispersion, a bright emission is collected only from the defect area (figure 7(a)). In order to extract the coherence of the 1D condensate, we used the same Mach–Zehnder interferometer in the center-symmetric configuration described in the previous section. This time, when phase matching only the 1D, the interference pattern is present only in the line-defect region (figure 7(b)). The corresponding coherence map presents a maximum degree of coherence of 0.5 at the center of the condensate, and decaying along the line direction, with a modulation ascribable to the fluctuations of the potential landscape (see figure 7(c)). To better visualize the spatial decay of the coherence, we present a cross-section of the coherence map (figure 8(a)), which demonstrates a fast decay of coherence along the defect direction dropping from the maximum value of 0.5 at the center

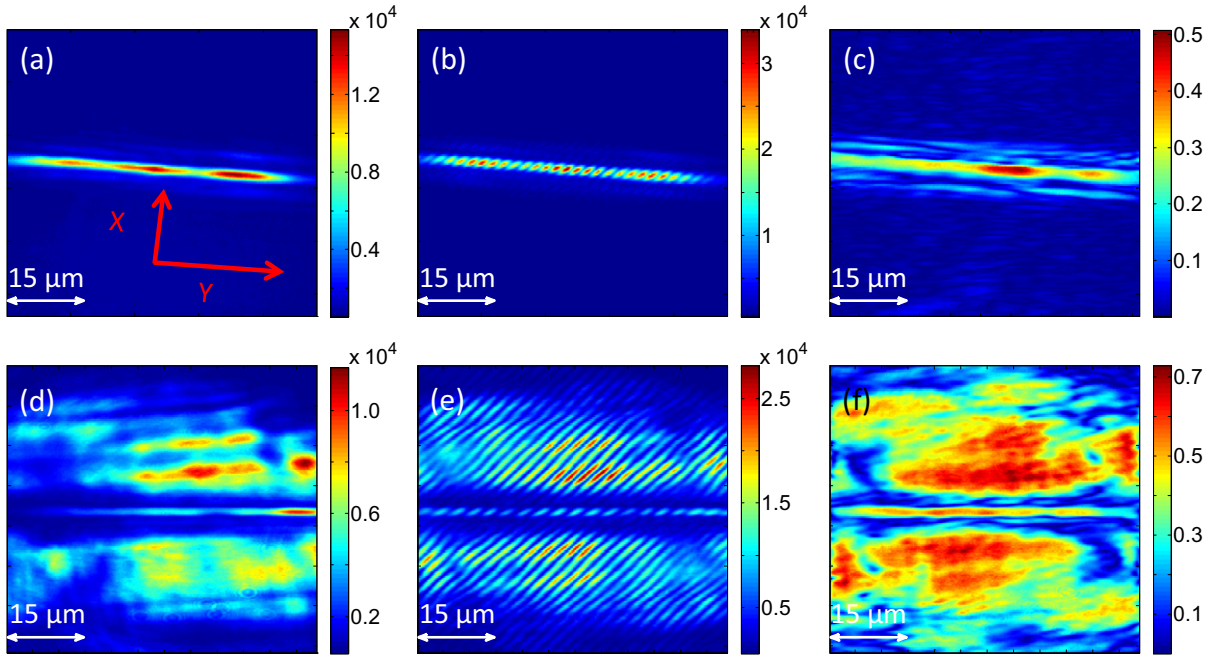

Figure 7. (a) Real-space emission from the line defect condensate, a corresponding interference pattern (b) and coherence map (c) when phase matching the line defect at $E_{\mathrm{Th}} = 1551.1$ meV and $P = 0.07$ W. (d) Real-space emission from the line defect condensate along with the 2D emission; a dark region of 6 μm separates the 2D and the 1D emission; the corresponding interference (e) and coherence map (f) when phase matching the 2D emission at $E_{\mathrm{Th}} = 1551.6$ meV and $P = 0.1$ W.

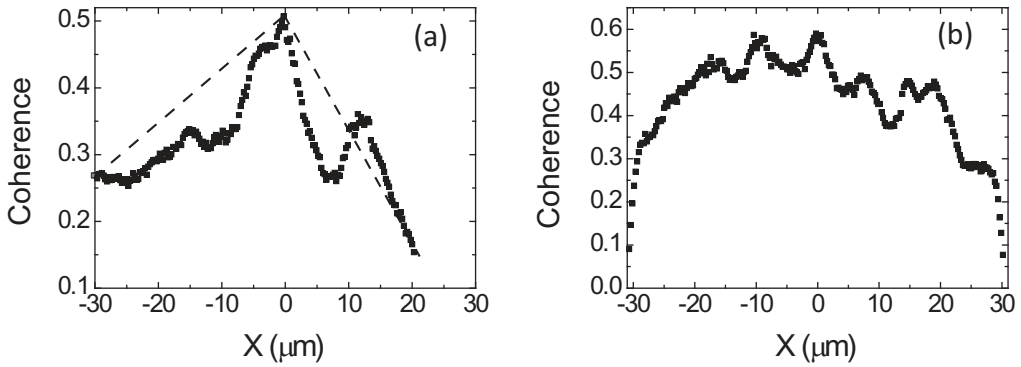

Figure 8. (a) Horizontal slice of the coherence map of the line defect presented in figure 7(c), showing a fast spatial decay modulated by the sample inhomogeneities (the dashed lines are a guide for the eye). (d) Horizontal slice of the coherence map of the line defect presented in figure 7(e), where higher degree of coherence and longer coherence length are reached, and with less dramatic effects of the sample inhomogeneities.

to 0.25 at a distance of only 10 μm. This result agrees qualitatively with the prediction of a decaying coherence in 1D systems presented in [25, 26]. From these data it is not possible to extract the predicted decaying law, because the coherence is modulated by the disorder of the sample. In fact, the reduced dimensionality makes the coherence more sensitive to the effects of sample disorder. A similar modulation of the spatial coherence along a line has already been observed for condensates created by non-resonant pumping in CdTe microcavities by Manni *et al* [29], who attributed the effect to disorder. It is worth mentioning that a very high and extended spatial coherence, lasting up to hundreds of microns, has been demonstrated in 1D systems by Wertz *et al* [30]. The observation of such coherence has been possible thanks to two main factors, i.e. the extremely high quality of the sample and the fact that they study, unlike us, propagating condensates which preserve their original spontaneous coherence during the propagation along the wire.

When, instead, the 2D system is phase matched, we observe in real space the coexistence of the emission from both the 2D and the line defect as shown in figure 7(d), with a dark region of about 6 μm separating them. The interference pattern presented in figure 7(e) reveals a higher contrast in the 2D region than that of the line defect region. It is worth noting that the fringes corresponding to the upper and the lower 2D part have the same orientation and periodicity, which indicates that the same phase is obtained in the two split 2D condensates, while the central region, where the line defect is located, presents fringes with a slightly different periodicity with respect to that of the 2D, which could be given by a different angle of emission. The coherence map presented in figure 7(f) reveals quite a large coherence modulated by the sample disorder in a less pronounced way. This is well evidenced in figure 8(b), where the horizontal profile of the coherence map of the line defect is shown. Under these conditions we observe an increase in the coherence length of the line defect as well; in this case two condensates are coexisting: one related to the 2D system created by parametric scattering and the other in the defect created by a sort of migration of polaritons from the 2D condensate toward the line defect, energetically favored by the lower energy of the 1D system.

It is well known that excitonic interactions lead to fluctuations in the number of particles in the condensate, and that these fluctuations broadening the energy of the emission are responsible for a faster decay of the coherence [28, 31]. To test the effect of interactions in the 1D system, we have also measured the temporal decay of the coherence when the OPO condensate is created only in the quasi-1D system. For this purpose we use the same setup employed for the spatial coherence measurements, this time measuring $g^{(1)}$ at a given point for different time delays τ, which permits the evaluation of the signal temporal coherence $g^{(1)}(\tau) = \frac{\langle E^*(t)E(t+\tau)\rangle}{\langle E^*(t)\rangle\langle E(t)\rangle}$. In this manner, we obtain $g^{(1)}$ from zero up to a maximum delay of $\sim$0.3 ns. A typical result of the temporal behavior of the coherence is presented in figure 9, where an exponentially decaying coherence is found. A fit of the data obtains a decay time of $\tau_c = 280$ ps, which is a long time compared to the polariton lifetime, but is almost an order of magnitude lower than the best value reported until now for 2D OPO polariton condensates [28]. We suggest that, as in the 2D case, this coherence time is limited by the interactions in the system [28]. However, converting it into a coherence length using the polariton mass would give a coherence length of the order of 100 μm, of the same order as those calculated in [26], but much longer than the coherence decay seen in figure 8(a). Thus we suggest that disorder is the dominant factor limiting the coherence decay in our experiments on 1D systems.

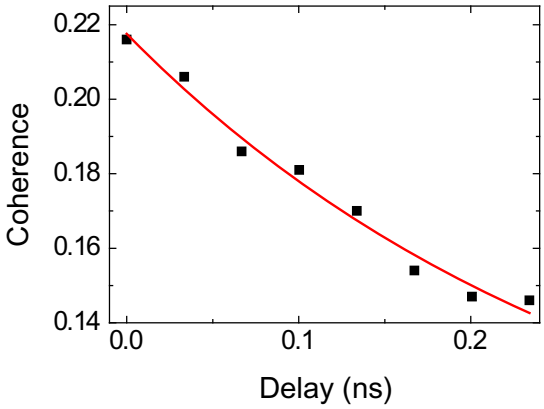

Figure 9. (a) Temporal coherence decay of the line defect condensate when phase matching the 1D system at $E_{\mathrm{Th}} = 1551.1$ meV. Each point of the curve corresponds to an average of points around the center of the line defect. A coherence decay time of $\tau_c = 280$ ps is extracted from fitting the experimental data with a monoexponential function.

4. Conclusions

In this work, we have given an overview of the coherence properties of polariton condensates generated by optical parametric scattering. The spatial coherence map of a 2D condensate has revealed the development of a constant phase along the entire condensate area. On the other hand, for an isolated 1D condensate we find that the coherence decays rapidly over length scales much smaller than our spot size. We also find a coherence time one order of magnitude smaller than that of a 2D condensate created in the same sample. Such a behavior may reflect the increasing importance of fluctuations as the dimensionality is reduced, as seen from theoretical work on non-equilibrium polariton condensates in the absence of disorder [25, 26] and as is familiar for both condensates and ordered phases in general. However, some of the effects may also relate to changes in the effective disorder strength.

Acknowledgments

The work was supported by the FP7 ITNs Clermont4 (235114) and Spin-optronics (237252), the Spanish MEC (MAT2011-22997), CAM (S-2009/ESP-1503) and Science Foundation Ireland SIRG/I1592 (PRE). We thank C Tejedor, I Carusotto and J Keeling for valuable discussions.

References

[1] Deveaud B (ed) 2007 *Physics of Semiconductor Microcavities: From Fundamentals to Nanoscale Devices* (Weinheim: Wiley-VCH)
[2] Kasprzak J *et al* 2006 *Nature* **443** 409
[3] Christopoulos S *et al* 2007 *Phys. Rev. Lett.* **98** 126405
[4] Amo A, Lefrére J, Pigeon S, Adrados C, Ciuti C, Carusotto I, Houdré R, Giacobino E and Bramati A 2009 *Nature Phys.* **5** 805
[5] Amo A *et al* 2009 *Nature* **457** 291

[6] Amo A *et al* 2011 *Science* **3** 1167
[7] Nardin G, Grosso G, Léger Y, Pietka B, Morier-Genoud F and Deveaud-Plédran B 2011 *Nature Phys.* **7** 635
[8] Sanvitto D *et al* 2010 *Nature Phys.* **6** 527
[9] Amo A, Liew T C H, Adrados C, Houdré R, Giacobino E, Kavokin A V and Bramati A 2010 *Nature Photonics* **4** 361
[10] Adrados C, Liew T C H, Amo A, Martín M D, Sanvitto D, Antón C, Giacobino E, Kavokin A, Bramati A and Viña L 2011 *Phys. Rev. Lett.* **107** 146402
[11] Paraiso T K, Wouters M, Léger Y, Morier-Genoud F and Deveaud-Plédran B 2010 *Nature Mater.* **9** 655
[12] Liew T C H, Shelykh I A and Malpuech G 2011 *Physica* E **43** 1543
[13] Stevenson R M, Astratov V N, Skolnick M S, Whittaker D M, Emam-Ismail M, Tartakovskii A I, Savvidis P G, Baumberg J J and Roberts J S 2000 *Phys. Rev. Lett.* **85** 3680
[14] Baumberg J J, Savvidis P G, Stevenson R M, Tartakovskii A I, Skolnick M S, Whittaker D M and Roberts J S 2000 *Phys. Rev.* B **62** R16248
[15] Baltes H P 1977 *Appl. Phys.* **12** 221
[16] Richard M, Wouters M and Dang L S 2010 Optical generation and control of quantum coherence in semiconductor nanostructures *Nanoscience and Technology* vol 146 ed G Slavcheva and P Roussignol (Berlin: Springer) chapter 11
[17] Pitaevskii L and Stringari S 2003 *Bose–Einstein Condensation* (Oxford: Oxford University Press)
[18] Penrose O and Onsager L 1956 *Phys. Rev.* **104** 576
[19] Baas A, Karr J Ph, Romanelli M, Bramati A and Giacobino E 2006 *Phys. Rev. Lett.* **96** 176401
[20] Krizhanovskii D N *et al* 2009 *Phys. Rev.* B **80** 045317
[21] Hadzibabic Z, Kruger P, Cheneau M, Battelier B and Dalibard J 2006 *Nature* **441** 1118
[22] Kavokin A and Malpuech G 2003 Cavity polaritons *Thin Films and Nanostructures* vol 32 ed V Agranovich and D Taylor (Amsterdam: Elsevier) chapter 5 pp 175–78
[23] Wouters M and Carusotto I 2007 *Phys. Rev.* A **76** 043807
[24] Ballarini D, Sanvitto D, Amo A, Viña L, Wouters M, Carusotto I, Lemaitre A and Bloch J 2009 *Phys. Rev. Lett.* **102** 056402
[25] Carusotto I and Ciuti C 2005 *Phys. Rev.* B **72** 125335
[26] Wouters M and Carusotto I 2006 *Phys. Rev.* B **74** 245316
[27] Malpuech G and Solnyshkov D 2012 arXiv:1204.2151v1
[28] Spano R, Cuadra J, Lingg C, Sanvitto D, Martin M D, Eastham P R, van der Poel M, Hvam J M and Viña L 2011 arXiv:1111.4894
[29] Manni F, Lagoudakis K G, Pietka B, Fontanesi L, Wouters M, Savona V, André R and Deveaud-Plédran B 2011 *Phys. Rev. Lett.* **106** 176401
[30] Wertz E *et al* 2010 *Nature Phys.* **6** 860
[31] Whittaker D M and Eastham P R 2009 *Europhys. Lett.* **87** 27002